Journal of Materials Chemistry C

ROYAL SOCIETY OF CHEMISTRY

COMMUNICATION

View Article Online
View Journal | View Issue

Cite this: J. Mater. Chem. C, 2022, 10, 13741

Received 14th April 2022,
Accepted 29th May 2022

DOI: 10.1039/d2tc01537d

rsc.li/materials-c

The influence of π–π stacking on the room temperature phosphorescence of phenothiazine 5,5-dioxide derivatives†

Jia Ren,[a] Yu Tian,[a] Yunsheng Wang,[a] Jie Yang,[a] Manman Fang *[a] and Zhen Li *[abcd]

The control of molecular packing in the aggregated state at the molecular design stage is significant but challenging. Herein, a strategy is provided to regulate the molecular packing as well as corresponding room temperature phosphorescence (RTP) performance. By changing the substituent, we designed five phenothiazine 5,5-dioxide derivatives to reveal their different RTP properties and inherent mechanism. Through careful analyses of experimental results, coupled with theoretical calculations, it is found that efficient intermolecular π–π interaction favors the long phosphorescence lifetime. Furthermore, polymorphisms with distinct intermolecular π–π interactions and RTP effects were obtained for compound PTZO-Cl, once again certifying the key role of strong π–π stacking in the persistent RTP effect. Also, these compounds with different RTP lifetimes were successfully utilized in silk-screen printing and multiple anti-counterfeiting.

Introduction

Recently, room temperature phosphorescence (RTP) luminogens have attracted considerable interest for their wide potential applications, such as organic light-emitting diodes (OLEDs), time-gated bioimaging, anti-counterfeiting and sensors.[1–11] In comparison with traditional inorganic materials or organic–metal complexes with the RTP effect, the pure organic ones show great advantages of low cost, good biocompatibility, easy preparation, *etc.*

Thanks to the enthusiasm of scientists, enumerable pure organic RTP systems have been successfully developed to explore their inherent mechanisms as well as corresponding applications. Systematic studies show that RTP effects in organic luminogens are heavily dependent on intermolecular interactions in the solid-state, such as H-aggregation, intermolecular n–π coupling, halogen bonding, hydrogen bonding, *etc.*[12–19] Besides, intermolecular π–π interaction in aggregates is also found to be much beneficial for the stabilization of triplet excitons and realization of persistent RTP. That is, the short distance and large overlap in the face-to-face π–π interactions could form the tight stacking of adjacent molecules, contributing to the prolonged phosphorescence lifetime.[20–25]

Herein, according to the previous works, we designed and synthesized a series of phenothiazine 5,5-dioxide derivatives, namely PTZO-CH_3O, PTZO-Br, PTZO-H, PTZO-F and PTZO-Cl. For these target compounds, the 1,2,3-trifluorophenyl group

[a] *Institute of Molecular Aggregation Science, Tianjin University, Tianjin 300072, China. E-mail: manmanfang@tju.edu.cn, lizhentju@tju.edu.cn, lizhen@whu.edu.cn; Tel: +86 181 0864 6953*
[b] *Department of Chemistry, Wuhan University, Wuhan 430072, China*
[c] *Joint School of National University of Singapore and Tianjin University, International Campus of Tianjin University, Binhai New City, Fuzhou 350207, China*
[d] *Wuhan National Laboratory for Optoelectronics, Huazhong University of Science and Technology, Wuhan 430074, China*

† Electronic supplementary information (ESI) available: Syntheses, photoluminescence behaviors, single crystal structures and structural characterizations. CCDC 2132708, 2132716, 2132713, 2132715, 2132714 and 2132717. For ESI and crystallographic data in CIF or other electronic format see DOI: https://doi.org/10.1039/d2tc01537d

Manman Fang

Manman Fang, received her PhD degree from Wuhan University in China under the supervision of Prof. Zhen Li in 2018. Then she joined Tianjin University (TJU) in July of 2018 as a lecturer. Her research interests mainly focus on the design and synthesis of new organic optoelectronic materials, including room temperature phosphorescence (RTP), mechanoluminescence (ML) and dye-sensitized solar cells (DSSCs). She has more than 10 publications as the first or corresponding author, including Prog. Mater. Sci., Angew. Chem. Int. Ed., Adv. Mater., J. Mater. Chem. C and so on.

was introduced to all of them to strengthen the intermolecular hydrogen bonding and inhibit the non-radiative transition, while the substituents in the 2-position of the phenothiazine 5,5-dioxide group were changed from each other, with the aim to accurately adjust the molecular packing and investigate the structure–packing–RTP property relationship.[26–28]

Excitingly, accompanying the adjustment of the substituent groups on the 2-position of the phenothiazine 5,5-dioxide ring from the methoxyl group to a bromine atom, and then to hydrogen, fluorine and chlorine atoms, the RTP lifetimes in crystals of the corresponding luminogens increased from 144 ms (PTZO-CH_3O) and 179 ms (PTZO-Br) to 332 ms (PTZO-H), and then to 446 ms (PTZO-F) and 745 ms (PTZO-Cl). Single crystal analyses indicated that the minor differences in the substituents could lead to much different intermolecular π–π interactions, thus resulting in the changed RTP properties. That is, the stronger the intermolecular π–π interaction, the longer the RTP lifetime. Surprisingly, we obtained another single-crystal of PTZO-Cl without the RTP effect, in which distinct molecular packing in a looser way (larger distance and small overlap for intermolecular π–π interactions) could be observed, further confirming that the compact packing is in favour of the stabilization of triplet excitons and realization of persistent RTP.

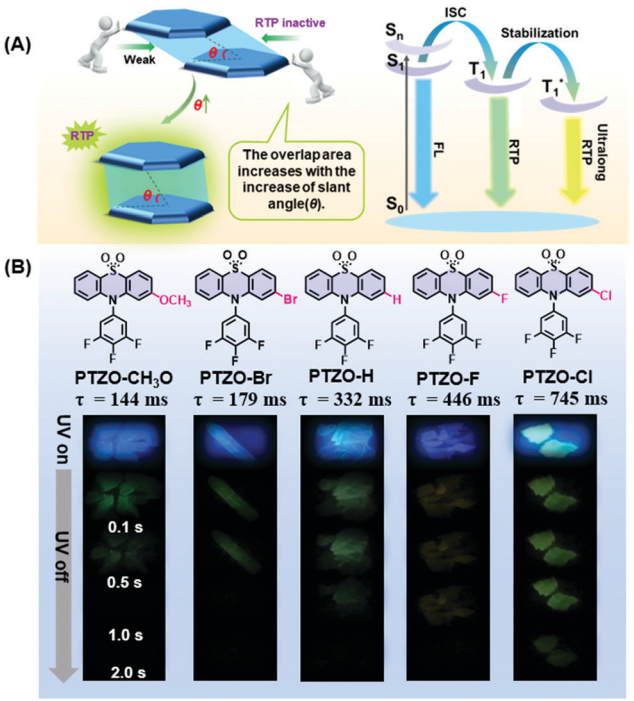

Fig. 1 (A) Strategy to promote the RTP performance. (B) Molecular structures of PTZO-CH_3O, PTZO-Br, PTZO-H, PTZO-F and PTZO-Cl, and their corresponding photographs were taken before and after turning off the 365 nm UV irradiation under ambient conditions.

Results and discussion

Five phenothiazine 5,5-dioxide derivatives of PTZO-CH_3O, PTZO-Br, PTZO-H, PTZO-F, and PTZO-Cl were designed by adjusting different substituents. The synthetic routes are described in Scheme S1 (ESI†). Their molecular structures and purity have been well confirmed by ^{1}H NMR, ^{13}C NMR, high-resolution mass spectra (HRMS), single-crystal X-ray diffraction (XRD), and high-performance liquid chromatography (HPLC). Then, their single crystals were cultured and corresponding photophysical properties were studied. Upon the illumination of a 365 nm ultraviolet (UV) lamp, their crystals showed blue or purple emissions. After stopping the excitation, green RTP emission lasting for more than 1.0 s could be visually seen for PTZO-H, PTZO-F, and PTZO-Cl, while those of PTZO-CH_3O and PTZO-Br would die out quickly (Fig. 1B). All of these phenomena were further confirmed by the steady-state photoluminescence (PL) spectra, phosphorescence spectra and corresponding lifetimes. As shown in Fig. 2A, the steady-state PL spectra of crystals displayed completely different profiles with emission peaks from 362 to 373 nm, whose lifetimes (τ_F) were measured to be about 1.21–2.82 ns, indicating the typical fluorescence character (Fig. S1, ESI†). Their PL quantum yields were also much different, from 0.22% to 2.55% in the crystal state (Table S1, ESI†). In the phosphorescence spectra, their emission peaks appeared from 500 nm to 515 nm, with lifetimes ranging from 144 to 745 ms (Fig. 2B). When the temperature decreased to 77 K, their lifetimes further increased, resulting in ultralong phosphorescence lifetimes of 0.63–1.81 s, since the cryogenic temperature can suppress the molecular

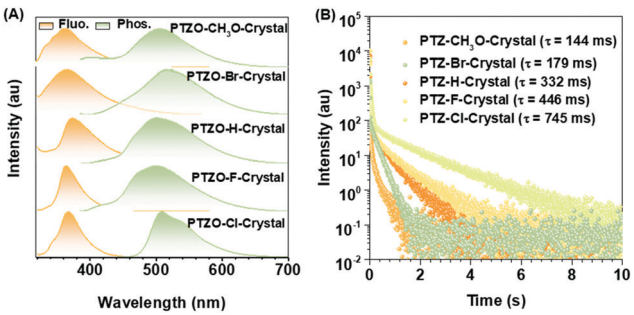

Fig. 2 (A) Normalized fluorescence (Orange line; λ_{ex} = 300 nm) and phosphorescence spectra (Green line; λ_{ex} = 365 nm) for PTZO-derivatives in the crystal state. (B) Room temperature phosphorescence decay curves of PTZO-derivatives in the crystal state.

motion to reduce the nonradiative rate (Fig. S2, ESI†). Thus, the prolonged lifetimes at low temperature further confirm the triplet feature of these emissions.

To study the origin of the different RTP performances for these five compounds, their UV-Vis absorption spectra were measured. The absorption spectra in dilute dichloromethane (DCM) solution are shown in Fig. S3A (ESI†), in which they have similar absorption bands at about 275, 300, and 330 nm, regardless of their different substituents. This indicates that the electronic effects of substituents have little effect on their energy levels. When it turns to a crystal state, much different absorption spectra can be observed, in which distinct

absorption peaks are presented (Fig. S3B, ESI†). In particular, the maximum absorption wavelength red-shifts from 330 nm (PTZO-Cl crystal) to 345 nm (PTZO-Br crystal), indicating their much different molecular packing in the crystal state. This could be further certified by the measurements of powder X-ray diffraction (PXRD), in which different PXRD patterns with sharp peaks could be observed for these five crystals (Fig. S4, ESI†). Also, the differential scanning calorimetry (DSC) measurements showed that these five target compounds had different melting points from 175.4 °C to 249.4 °C, due to their different molecular structures and intermolecular interactions in crystals (Fig. S5, ESI†). Thus, regardless of the similar molecular structure for these five target compounds, much different molecular packing could be obtained, which then affects the corresponding photophysical properties, including the RTP effect.

In order to further investigate the relationship between luminescent behaviour and molecular packing, their single crystal structures were measured, and the dimers formed by adjacent molecules were extracted from the crystals for detailed analysis (Table S2 and Fig. S6–S8, ESI†). Fig. 3 shows the entire and local packing modes of these crystals, which are different from each other corresponding to the subtly different substituent groups on the 2-position of the phenothiazine 5,5-dioxide ring.

In detail, PTZO-CH_3O and PTZO-Br crystals present the space groups of $P12_1/c1$ and $R\bar{3}$. Among them, the distance (d) and slant angle (θ) of the molecular dimer in the PTZO-CH_3O crystal is 3.51 Å and 60.0° respectively, while they are 3.41 Å and 58.0° for PTZO-Br. Interestingly, the crystals of PTZO-H, PTZO-F and PTZO-Cl exhibit almost similar molecular packing modes with the same space group of Pbca, which will be much beneficial for analyzing their intermolecular interactions. For these three crystals, the main differences also exist in their intermolecular distance (d) and slant angle (θ) within the molecular dimer. As we can see, the intermolecular distance (d) of the molecular dimer decreases gradually from 3.62 Å (PTZO-H and PTZO-F) to 3.61 Å (PTZO-Cl), while the corresponding slant angle (θ) increases from 66.9° (PTZO-H) and 67.9° (PTZO-F) to 69.0° (PTZO-Cl). This indicates the gradually enhanced intermolecular π–π interactions in crystals are consistent with their prolonged RTP lifetimes. Besides, although the intermolecular distances of PTZO-H, PTZO-F and PTZO-Cl dimers were a little longer than those of PTZO-CH_3O and PTZO-Br, the corresponding slant angles were all larger than PTZO-CH_3O and PTZO-Br crystals, meaning the increased overlap between adjacent molecules with a face-to-face arrangement. Then, the larger π–π overlaps lead to the much longer RTP lifetimes of PTZO-H, PTZO-F and PTZO-Cl crystals than PTZO-CH_3O and PTZO-Br.

From the above analyses, it can be concluded that the minor difference in substituent could lead to a significant change in intermolecular π–π interactions, including intermolecular distance (d) and slant angle (θ). Among them, the PTZO-Cl crystal takes the largest π–π overlap in the molecular dimer with the slant angle of 69.0°, thus enhancing the intermolecular

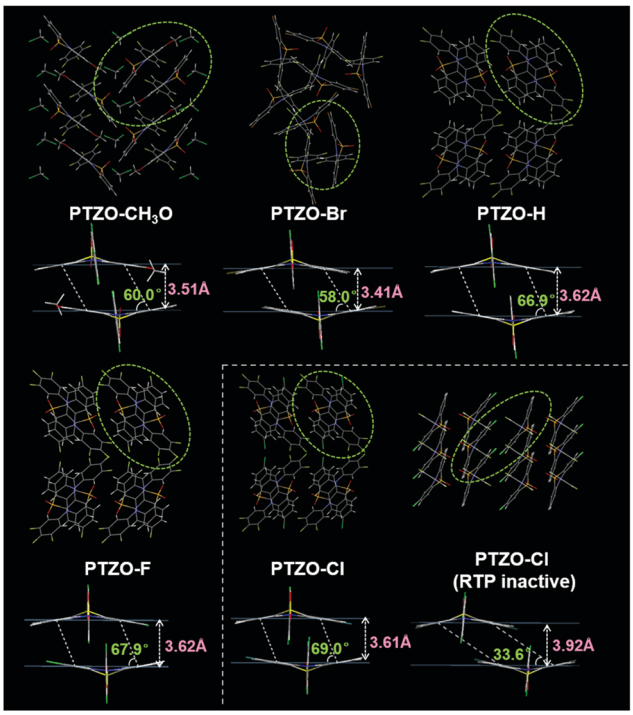

Fig. 3 Single-crystal structures of the five target compounds. Entire and local packing modes of the crystals for PTZO-CH_3O, PTZO-Br, PTZO-H, PTZO-F, PTZO-Cl and PTZO-Cl (RTP inactive). The local packing pictures are selected from the parts in cycles of corresponding entire ones, in which the plane–plane distances and the slant angles of the involved planes are listed.

interactions and leading to the longest RTP lifetime of 745 ms. For other compounds, the changes in intermolecular π–π interactions with the different slant angles are also in good accordance with their changing tendency of RTP lifetimes in crystals. That is, the larger the π–π overlap, the longer the RTP lifetime, demonstrating the significant role of intermolecular π–π stacking in the RTP effect. Therefore, when dissolving them in DCM solution, no RTP could be detected. Only at low temperature (77 K), the phosphorescence could be observed for the largely restricted non-radiative transition (Fig. S9 and S10, ESI†).

Surprisingly, we obtained another single crystal of PTZO-Cl, named PTZO-Cl (RTP-inactive), by changing the culture conditions. As easily seen in Fig. S11 (ESI†), different from the PTZO-Cl crystal with the RTP effect, the PTZO-Cl (RTP-inactive) one is RTP inactive and its PL quantum yield is just 0.94% (Table S1, ESI†). Single X-ray diffraction (XRD) analyses show that PTZO-Cl (RTP inactive) crystal presents another type of space group of $P12_1/c1$ (Table S2, ESI†). Also, its molecular dimer shows much weaker intermolecular π–π interactions with the small intermolecular overlap (θ = 33.6°) and large intermolecular distance (d) of 3.92 Å (Fig. 3). Even compared to PTZO-CH_3O, PTZO-Br, PTZO-H and PTZO-F crystals, the π–π interactions of the PTZO-Cl (RTP inactive) crystal are also much weaker, thus resulting in its non-RTP effect. Besides, the powder XRD patterns could also certify the different molecular packing

between PTZO-Cl and PTZO-Cl (RTP inactive) crystals. As shown in Fig. S12 (ESI†), PTZO-Cl (RTP inactive) shows sharp peaks at about 7° and 22°, while the PTZO-Cl crystal with the RTP effect has sharp peaks at about 8°, 23° and 31°. These data certify the significant role of intermolecular π–π interactions in the RTP effect of phenothiazine 5,5-dioxide derivatives. To further prove this, the RTP performance of PTZO-Cl ground powder was measured. After grinding, the RTP intensity of PTZO-Cl decreased sharply and the lifetime was shortened from 745 to 31 ms, as the mechanical stimulus had destroyed the intermolecular π–π interactions in the solid-state (Fig. S13, ESI†). Further on, when PTZO-Cl was doped into a polymethyl methacrylate (PMMA) matrix with a mass ratio of 1%, no RTP could be detected, which demonstrates the significant role of intermolecular π–π interactions in the RTP effect again (Fig. S14, ESI†).

Furthermore, TD-DFT calculations were carried out to study the relationship between molecular packing and the RTP effect. We first performed calculations of the highest occupied molecular orbital (HOMO) and lowest unoccupied molecular orbital (LUMO) to investigate the nature of the excitation in these dimers from single crystals. Taking the two polymorphisms of PTZO-Cl as examples, the electron clouds of HOMO and LUMO are both located on the phenothiazine 5,5-dioxide ring, indicating that it acts as the main luminophore.[29] Interestingly, obvious electron communication could be observed for the adjacent parallel phenothiazine 5,5-dioxide ring in the LUMO orbital, which would surely affect the resultant luminescent behaviours, including RTP emission. Additionally, reduced density gradient (RDG) analyses revealing the intermolecular interactions were carried out, in which the blue region indicates attractive interactions, the green region is for van der Waals and the brown region is for steric hindrance (Fig. 4B). The larger green or brown-green isosurface within the molecular dimer in the PTZO-Cl crystal suggests its stronger intermolecular π–π interaction than the PTZO-Cl (RTP inactive) crystal. Also, in the scatter diagrams of the RDG analysis, there are more spikes in the range of −0.01 to 0.01 a.u. of the sign(I_2)r function for the PTZO-Cl crystal, further verifying the stronger π–π interactions in it, which then contributes much to the resultant ultralong RTP emission.[30,31] Thus, the existence of efficient intermolecular π–π interaction and its significant influence on RTP emission could be further certified based on these theoretical calculations.

To fully utilize the ultralong lifetime of these organic RTP luminogens, the applications of time-resolved anti-counterfeiting were explored. Firstly, PTZO-Cl with the longest RTP lifetime was utilized to prepare a two-dimensional code through simple screen printing.[32–36] The anti-counterfeiting ink was prepared by dispersing the PTZO-Cl powder in ALOE VERA gel. Then, a two-dimensional code was printed on a piece of filter paper by using this special ink. Under natural light, the screen-printing pattern was invisible, as depicted in Fig. 5A. However, after UV irradiation, the two-dimensional code with green afterglow could be clearly observed by the naked eye. Furthermore, when the polyvinyl alcohol (PVA) film of fluorescein was covered on the screen-printing pattern, it would be invisible under UV irradiation due to the interference of strong

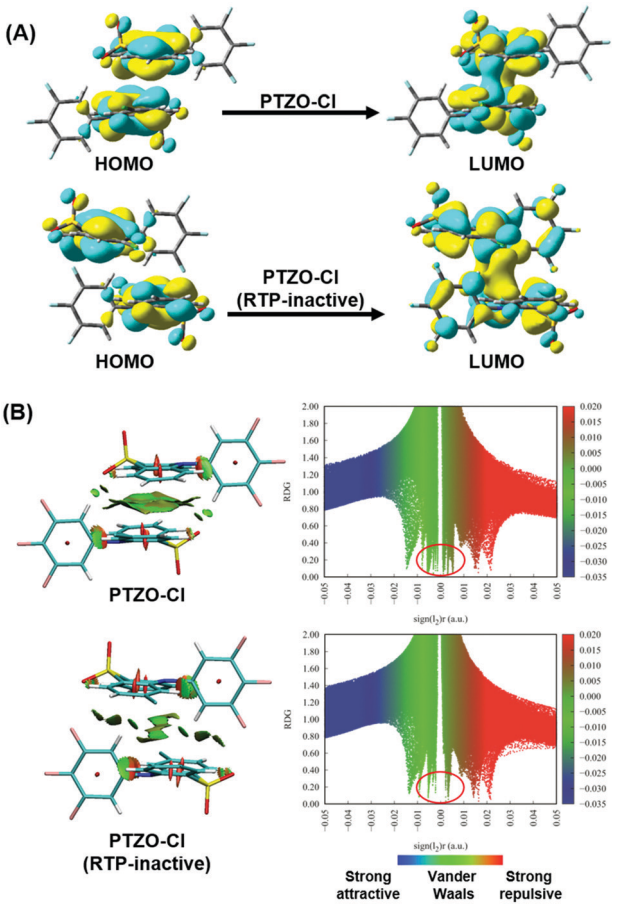

Fig. 4 (A) HOMO/LUMO orbital distributions of the molecular dimers of PTZO-Cl and PTZO-Cl (RTP-inactive). (B) Distributions of intermolecular interaction regions in molecular dimers of PTZO-Cl and PTZO-Cl (RTP-inactive).

green fluorescence from fluorescein. However, the two-dimensional code could be observed after stopping the UV irradiation for the long RTP lifetime of PTZO-Cl, which could serve as a great addition to the traditional anti-counterfeiting technology based on fluorescence (Fig. S11, ESI†).

Then, in consideration of the different RTP performances of PTZO-CH_3O, PTZO-Br, PTZO-H, PTZO-F and PTZO-Cl, the multiple security protection with color mode and time-resolved mode was explored. As shown in Fig. 5B, the pattern of the cloud was filled with PTZO-Cl powder, which showed green emission under UV irradiation. Then, the raindrop patterns were filled in with PTZO-CH_3O, PTZO-H and PTZO-Br powders in order. Finally, PTZO-F powder was used to fabricate a star with purple emission. After turning off the UV irradiation suddenly, the cloud, star and the centre raindrop with the ultralong green RTP could be readily visualized, while the other parts with shorter RTP emissions couldn't. After a while, the raindrop gradually disappeared, and the cloud and star shaded in turn with time prolonged. This process at room temperature without any other external stimulation makes these compounds promising candidates for multiple anti-counterfeiting security protection materials.

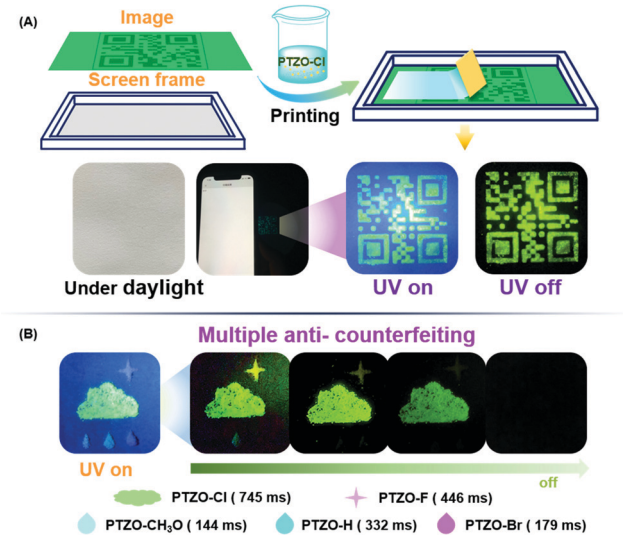

Fig. 5 (A) The schematic diagram of the screen-printing process and the two-dimensional code which could be identified by cell phone. (B) Multiple security protection applications by using five kinds of components of prepared powders of PTZO-CH_3O (the left raindrop), PTZO-Br (the right raindrop), PTZO-H (the middle raindrop), PTZO-F (the star), and PTZO-Cl (the cloud).

Conclusions

In summary, we designed and synthesized five phenothiazine 5,5-dioxide derivatives containing different substituents, which demonstrate different phosphorescence properties at room temperature. Through experimental analyses and theoretical calculations, it is demonstrated that efficient intermolecular π–π interaction, especially for the large π–π overlap with the molecular dimer, is beneficial for the persistent RTP effect. The two polymorphisms of PTZO-Cl with totally different RTP effects could further certify this point, further demonstrating the Molecular Uniting Set Identified Characteristic (MUSIC).[37–55] In addition, a series of anti-counterfeiting applications were demonstrated, based on their distinct RTP effects. This study provides an effective strategy for regulating and controlling the intermolecular interactions of π systems, giving some new insights into the structure–packing–performance relationship of functional materials.

Conflicts of interest

There are no conflicts to declare.

Acknowledgements

This work was supported by the National Natural Science Foundation of China (No. 21905197), the starting grants of Tianjin University and Tianjin Government, and the Open Project Program of Wuhan National Laboratory for Optoelectronics (No. 2020WNLOKF013).

Notes and references

1 R. Kabe, N. Notsuka, K. Yoshida and C. Adachi, *Adv. Mater.*, 2016, **28**, 655–660.
2 D. Lee, O. Bolton, B. Kim, J. Youk, S. Takayama and J. Kim, *J. Am. Chem. Soc.*, 2013, **135**, 6325–6329.
3 J. Zhi, Q. Zhou, H. Shi, Z. An and W. Huang, *Chem. – Asian J.*, 2020, **15**, 947–957.
4 Y. Tian, J. Yang, Z. Liu, M. Gao, X. Li, W. Che, M. Fang and Z. Li, *Angew. Chem., Int. Ed.*, 2021, **60**, 20259–20263.
5 S. Fateminia, Z. Mao, S. Xu, Z. Yang, Z. Chi and B. Liu, *Angew. Chem., Int. Ed.*, 2017, **56**, 12160–12164.
6 Y. Wang, H. Gao, J. Yang, M. Fang, D. Ding, B. Tang and Z. Li, *Adv. Mater.*, 2021, **33**, 2007811.
7 Y. Wang, J. Yang, M. Fang, Y. Gong, J. Ren, L. Tu, B. Tang and Z. Li, *Adv. Funct. Mater.*, 2021, **31**, 2101719.
8 D. Li, J. Yang, M. Fang, B. Tang and Z. Li, *Sci. Adv.*, 2022, **8**, eabl8392.
9 S. Xu, R. Chen, C. Zheng and W. Huang, *Adv. Mater.*, 2016, **28**, 9920–9940.
10 S. Mukherjee and P. Thilagar, *Chem. Commun.*, 2015, **51**, 10988–11003.
11 Kenry, C. Chen and B. Liu, *Nat. Commun.*, 2019, **10**, 2111.
12 P. Alam, T. Cheung, N. Leung, J. Zhang, J. Guo, L. Du, R. Kwok, J. Lam, Z. Zeng, D. Phillips, H. Sung, I. Williams and B. Tang, *J. Am. Chem. Soc.*, 2022, **144**, 3050–3062.
13 Y. Gong, S. He, Y. Li, Z. Li, Q. Liao, Y. Gu, J. Wang, B. Zou, Q. Li and Z. Li, *Adv. Opt. Mater.*, 2020, **8**, 1902036.
14 Q. Liao, Q. Gao, J. Wang, Y. Gong, Q. Peng, Y. Tian, Y. Fan, H. Guo, D. Ding, Q. Li and Z. Li, *Angew. Chem., Int. Ed.*, 2020, **59**, 9946–9951.
15 S. Cai, H. Shi, Z. Zhang, X. Wang, H. Ma, N. Gan, Q. Wu, Z. Cheng, K. Ling, M. Gu, C. Ma, L. Gu, Z. An and W. Huang, *Angew. Chem., Int. Ed.*, 2018, **57**, 4005–4009.
16 E. Hamzehpoor and D. Perepichka, *Angew. Chem., Int. Ed.*, 2020, **59**, 9977–9981.
17 Y. Shoji, Y. Ikabata, Q. Wang, D. Nemoto, A. Sakamoto, N. Tanaka, J. Seino, H. Nakai and T. Fukushima, *J. Am. Chem. Soc.*, 2017, **139**, 2728–2733.
18 O. Bolton, K. Lee, H. Kim, K. Lin and J. Kim, *Nat. Chem.*, 2011, **3**, 205–210.
19 Z. An, C. Zheng, Y. Tao, R. Chen, H. Shi, T. Chen, Z. Wang, H. Li, R. Deng, X. Liu and W. Huang, *Nat. Mater.*, 2015, **14**, 685–690.
20 Q. Li, Y. Tang, W. Hu and Z. Li, *Small*, 2018, **14**, 1801560.
21 X. Wang, W. Guo, H. Xiao, Q. Yang, B. Chen, Y. Chen, C. Tung and L. Wu, *Adv. Funct. Mater.*, 2020, **30**, 1907282.
22 Z. Ruan, Q. Liao, Q. Dang, X. Chen, C. Deng, Z. Gao, J. Lin, S. Liu, Y. Chen, Z. Tian and Z. Li, *Adv. Opt. Mater.*, 2021, **9**, 2001549.
23 Q. Li and Z. Li, *Adv. Sci.*, 2017, **4**, 1600484.
24 Y. Tian, Y. Gong, Q. Liao, Y. Wang, J. Ren, M. Fang, J. Yang and Z. Li, *Cell Rep. Phys. Sci.*, 2020, **1**, 100052.
25 Q. Guo, S. Zhou, X. Li, L. Tao, M. Li, S. Su, D. Wan and J. Li, *Chem. Commun.*, 2021, **57**, 6177–6180.
26 J. Yang, M. Fang and Z. Li, *Acc. Mater. Res.*, 2021, **2**, 644–654.

27 J. Yang, X. Zhen, B. Wang, X. Gao, Z. Ren, J. Wang, Y. Xie, J. Li, Q. Peng, K. Pu and Z. Li, *Nat. Commun.*, 2018, **9**, 840.
28 J. Ren, Y. Wang, Y. Tian, Z. Liu, X. Xiao, J. Yang, M. Fang and Z. Li, *Angew. Chem., Int. Ed.*, 2021, **133**, 12443–12448.
29 J. Zhang, S. Mukamel and J. Jiang, *J. Phys. Chem. B*, 2020, **124**, 2238–2244.
30 Z. Mao, Z. Yang, C. Xu, Z. Xie, L. Jiang, F. Gu, J. Zhao, Y. Zhang, M. Aldreda and Z. Chi, *Chem. Sci.*, 2019, **10**, 7352–7357.
31 J. Wu, J. Liu, S. Yuan, Z. Wang, J. Zhou and K. Cen, *Energy Fuels*, 2016, **30**, 7118–7124.
32 Y. Miao, S. Liu, L. Ma, W. Yang, J. Li and J. Lv, *Anal. Chem.*, 2021, **93**, 4075–4083.
33 Y. Zhang, H. Yang, H. Ma, G. Bian, Q. Zang, J. Sun, C. Zhang, Z. An and W. Wong, *Angew. Chem., Int. Ed.*, 2019, **58**, 8773–8778.
34 L. Gu, H. Shi, L. Bian, M. Gu, K. Ling, X. Wang, H. Ma, S. Cai, W. Ning1, L. Fu, H. Wang, S. Wang, Y. Gao, W. Yao, F. Huo, Y. Tao, Z. An, X. Liu and W. Huang, *Nat. Photonics*, 2019, **13**, 406–411.
35 Y. Yang, J. Wang, D. Li, J. Yang, M. Fang and Z. Li, *Adv. Mater.*, 2021, **33**, 2104002.
36 D. Li, Y. Yang, J. Yang, M. Fang, B. Tang and Z. Li, *Nat. Commun.*, 2022, **13**, 347.
37 M. Fang, J. Yang and Z. Li, *Prog. Mater. Sci.*, 2022, **125**, 100914.
38 Y. Xie and Z. Li, *Natl. Sci. Rev.*, 2021, **8**, nwaa199.
39 J. Wang, Q. Dang, Y. Gong, Q. Liao, G. Song, Q. Li and Z. Li, *CCS Chem.*, 2021, **3**, 274–286.
40 R. Tang, S. Zhou, Z. Cheng, H. Chen, L. Deng, Q. Peng and Z. Li, *CCS Chem.*, 2020, **2**, 1040–1048.
41 S. Li, Y. Xie, A. Li, X. Li, W. Che, J. Wang, H. Shi and Z. Li, *Sci. China Mater.*, 2021, **64**, 2813–2823.
42 L. Tu, Y. Xie, Z. Li and B. Tang, *SmartMat.*, 2021, **2**, 326–346.
43 Y. Yang, J. Yang, M. Fang and Z. Li, *Chem. Res. Chin. Univ.*, 2021, **37**, 598–614.
44 M. Jin, Z. Zhu, Q. Liao, Q. Li and Z. Li, *Chinese J. Polym. Sci.*, 2020, **38**, 118–125.
45 Q. Li and Z. Li, *Acc. Chem. Res.*, 2020, **53**, 962–973.
46 J. Yang, M. Fang and Z. Li, *Aggregate*, 2020, **1**, 6–18.
47 F. Liu, Q. Liao, J. Wang, Y. Gong, Q. Dang, W. Ling, M. Han, Q. Li and Z. Li, *Sci. China: Chem.*, 2020, **63**, 1435–1442.
48 Q. Li and Z. Li, *Sci. China Mater.*, 2020, **63**, 177–184.
49 J. Wang and Z. Li, *Acta. Chim. Sin.*, 2021, **79**, 575–587.
50 K. Chang, Q. Li and Z. Li, *Chinese. J. Org. Chem.*, 2020, **40**, 3656–3671.
51 Y. Li, F. Gu, B. Ding, L. Zou and X. Ma, *Sci. China: Chem.*, 2021, **64**, 1297–1301.
52 J. Yang, M. Fang and Z. Li, *InfoMat*, 2020, **2**, 791–806.
53 Y. Wang, J. Yang, Y. Gong, M. Fang, Z. Li and B. Tang, *SmartMat.*, 2020, **1**, e1006.
54 Y. Fan, S. Liu, M. Wu, L. Xiao, Y. Fan, M. Han, K. Chang, Y. Zhang, X. Zhen, Q. Li and Z. Li, *Adv. Mater.*, 2022, **34**, 202201280.
55 Y. Tian, X. Yang, Y. Gong, Y. Wang, M. Fang, J. Yang, Z. Tang and Z. Li, *Sci. China: Chem.*, 2021, **64**, 445–451.

